Chemistry–A European Journal

Supporting Information

Endohedral Hydrogen Bonding Templates the Formation of a Highly Strained Covalent Organic Cage Compound**

Natalie Schäfer,[a, b] Michael Bühler,[b] Lisa Heyer,[a, b] Merle I. S. Röhr,[b] and Florian Beuerle*[a, b]

Content

1 Synthetic Procedures

Compounds **S2**,[S1] **3**,[S2] **4**,[S1] **5**[S3] and **A**[S4] have been synthesized according to previously published procedures.

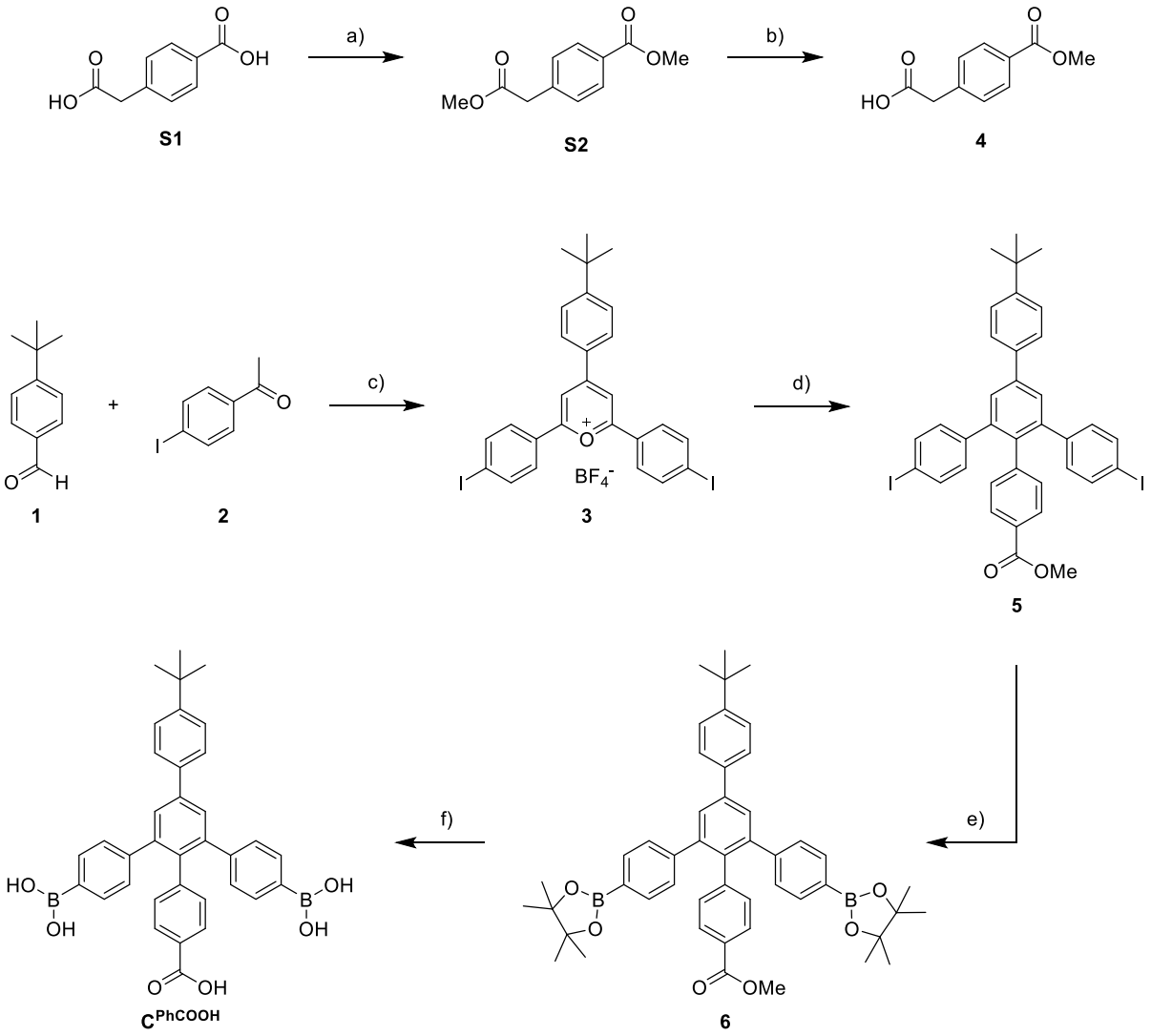

Scheme S1. Synthesis of diboronic acid $\mathbf{C}^{\mathbf{PhCOOH}}$: a) H_2SO_4, MeOH, 90 °C, 19 h, 93%, b) K_2CO_3, MeOH/H_2O, rt, 24 h, 93%, c) $BF_3 \cdot OEt_2$, 100 °C, 2 h, 38%, d) 1. **4**, NaOH, MeOH, 30 min, 2. Ac_2O, 160 °C, 2 h, 55%, e) B_2pin_2 / KOAc / $Pd(dppf)Cl_2$, DMF, reflux, 2 h 30 min, 71%, f) BBr_3, CH_2Cl_2, 3 h 45 min, 0 °C → rt, 76%.

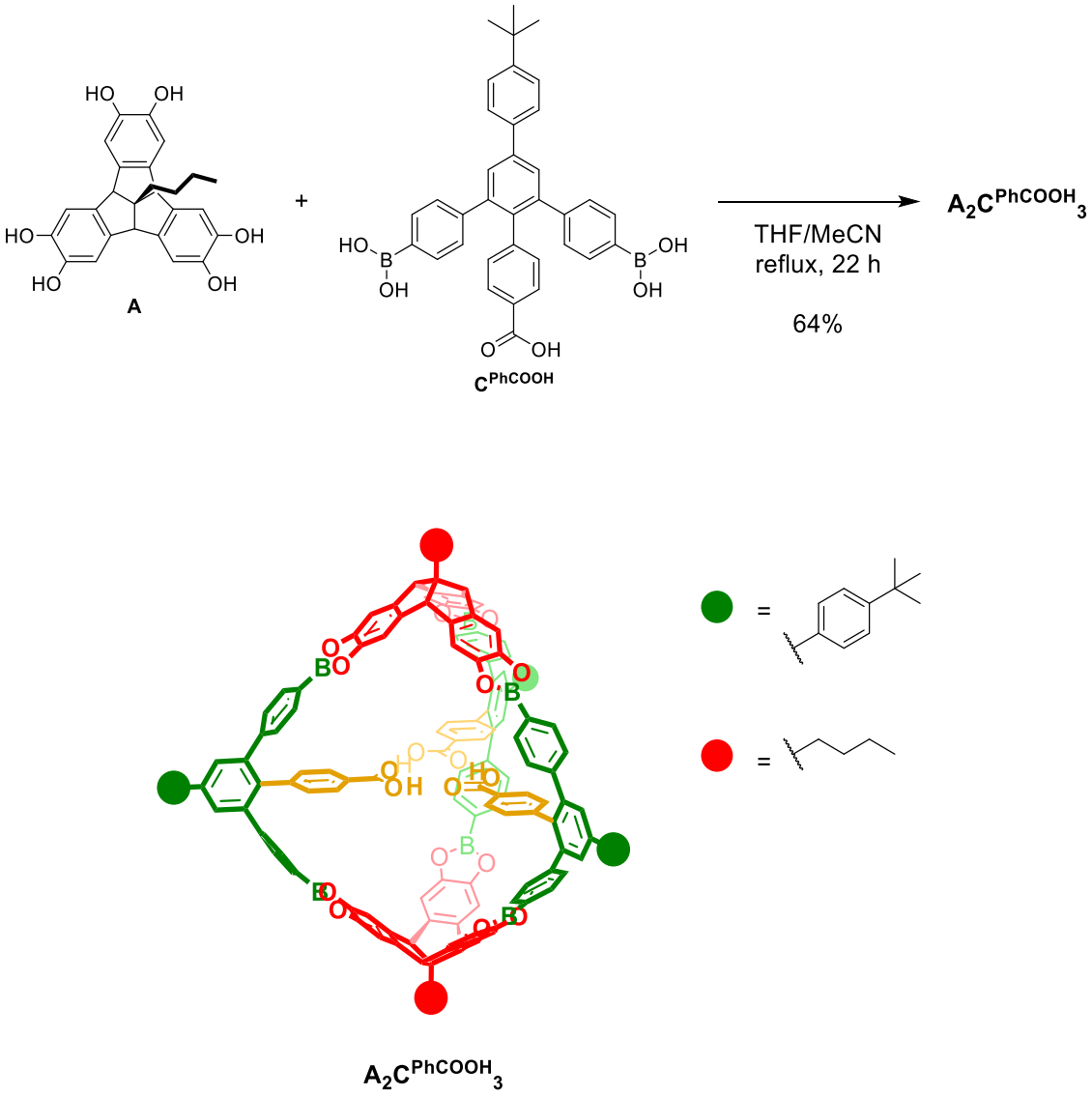

Scheme S2. Synthesis of cage $\mathbf{A_2C^{PhCOOH}_3}$.

2 Analytical Data

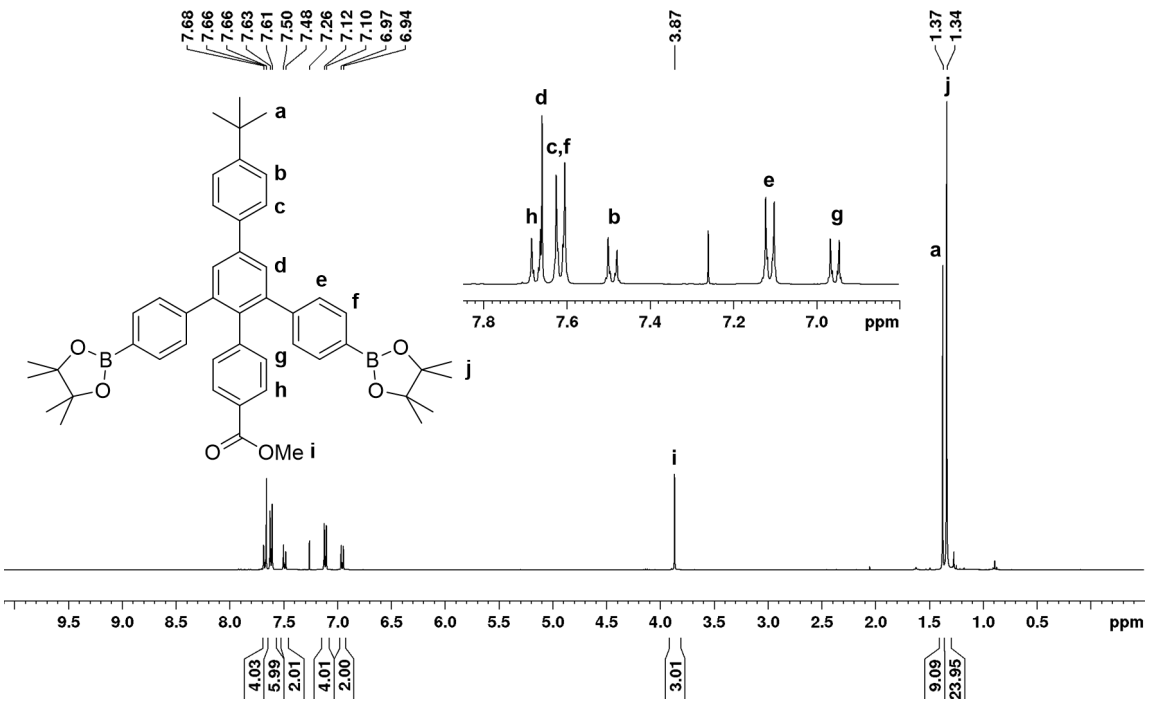

Figure S1. ^{1}H NMR (400 MHz, $CDCl_3$, rt) spectrum of **6**.

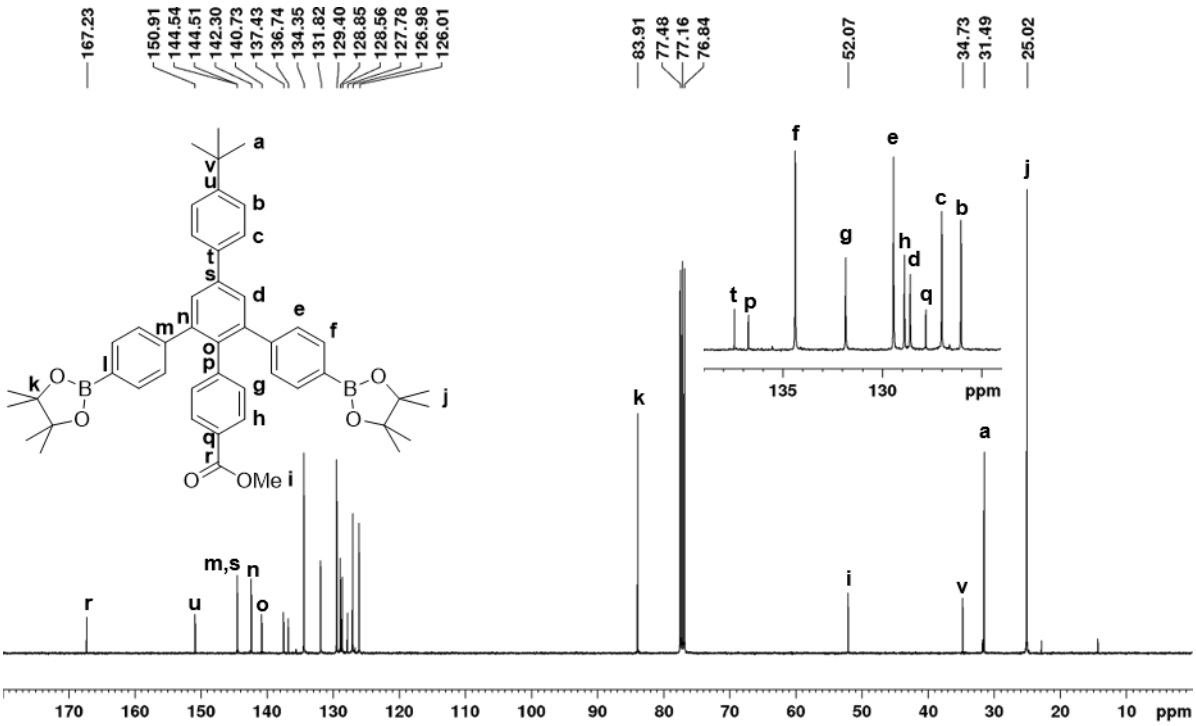

Figure S2. ^{13}C NMR (101 MHz, $CDCl_3$, rt) spectrum of **6**.

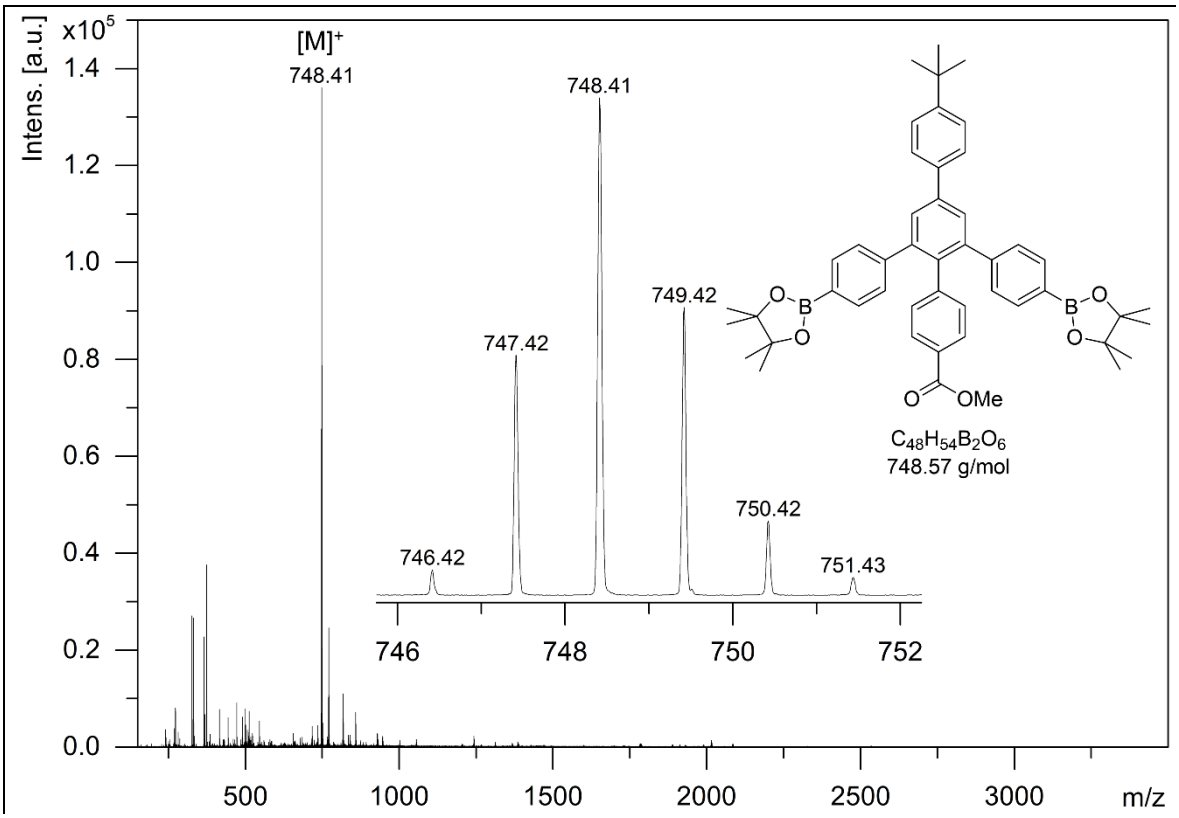

Figure S3. MS (MALDI-TOF, DCTB in $CHCl_3$, pos.) of **6**.

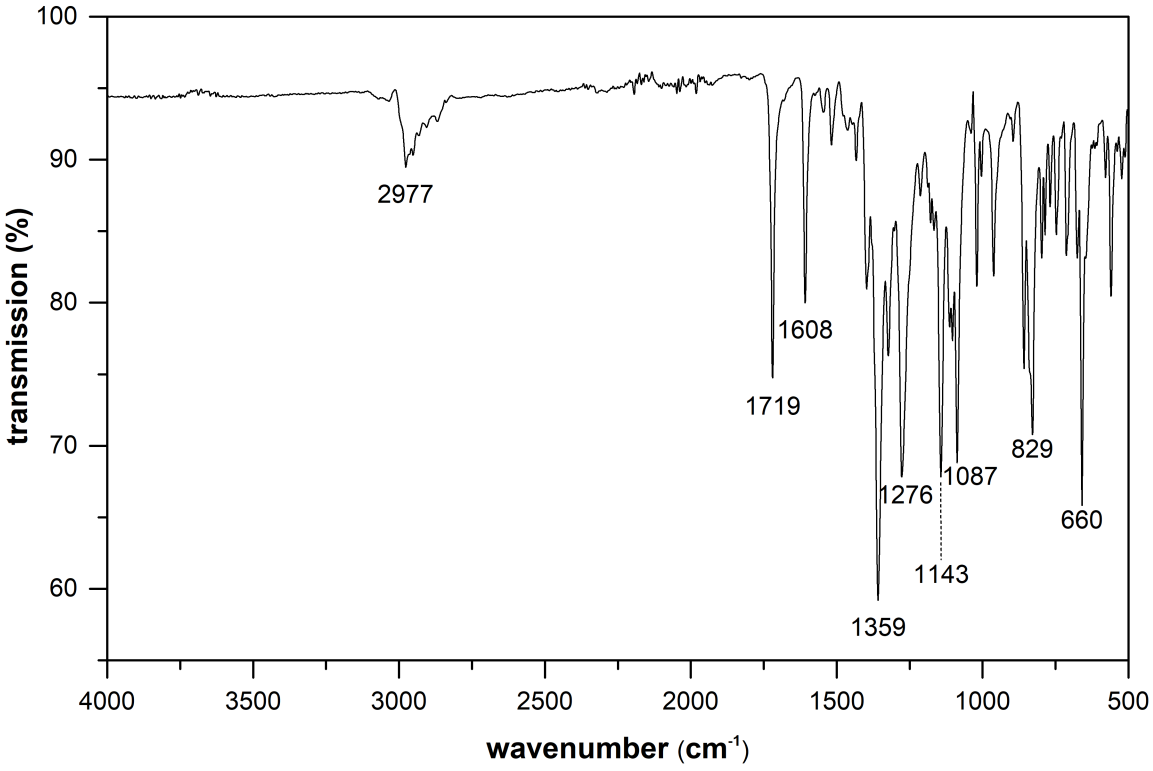

Figure S4. FT-IR spectrum of **6**.

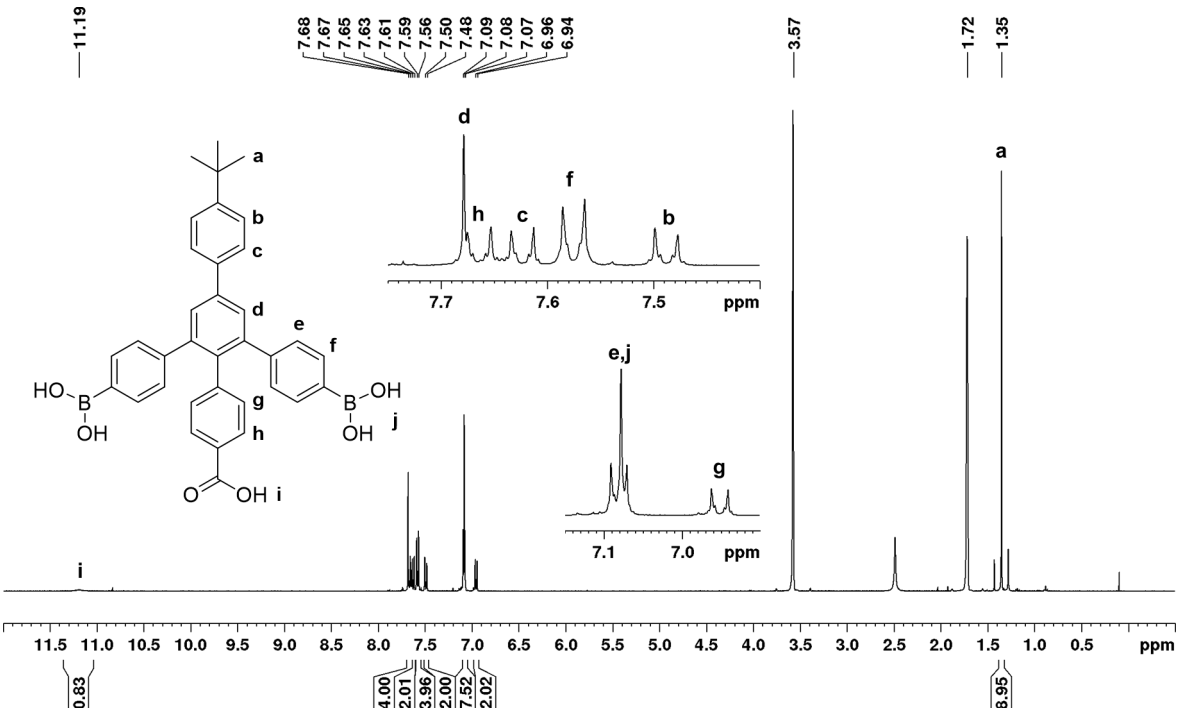

Figure S5. ^{1}H NMR (400 MHz, THF-d_8, rt) spectrum of $\mathbf{C}^{\mathbf{PhCOOH}}$.

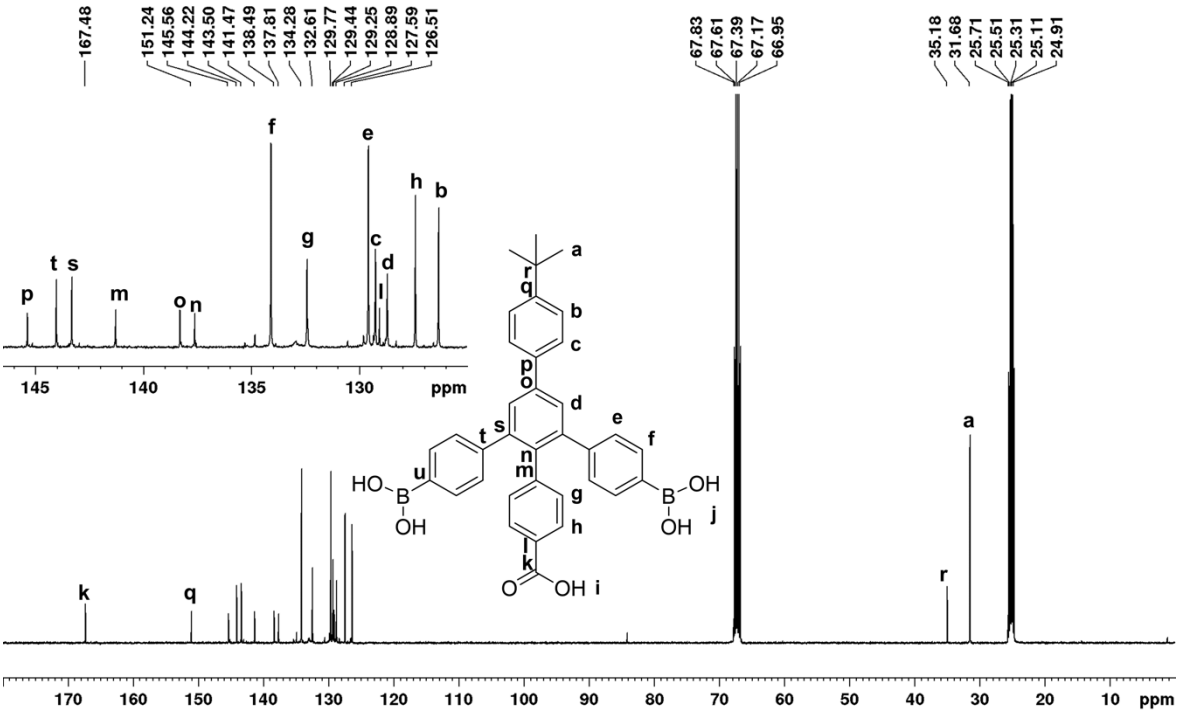

Figure S6. ^{13}C NMR (101 MHz, THF-d_8, rt) spectrum of $\mathbf{C}^{\mathbf{PhCOOH}}$.

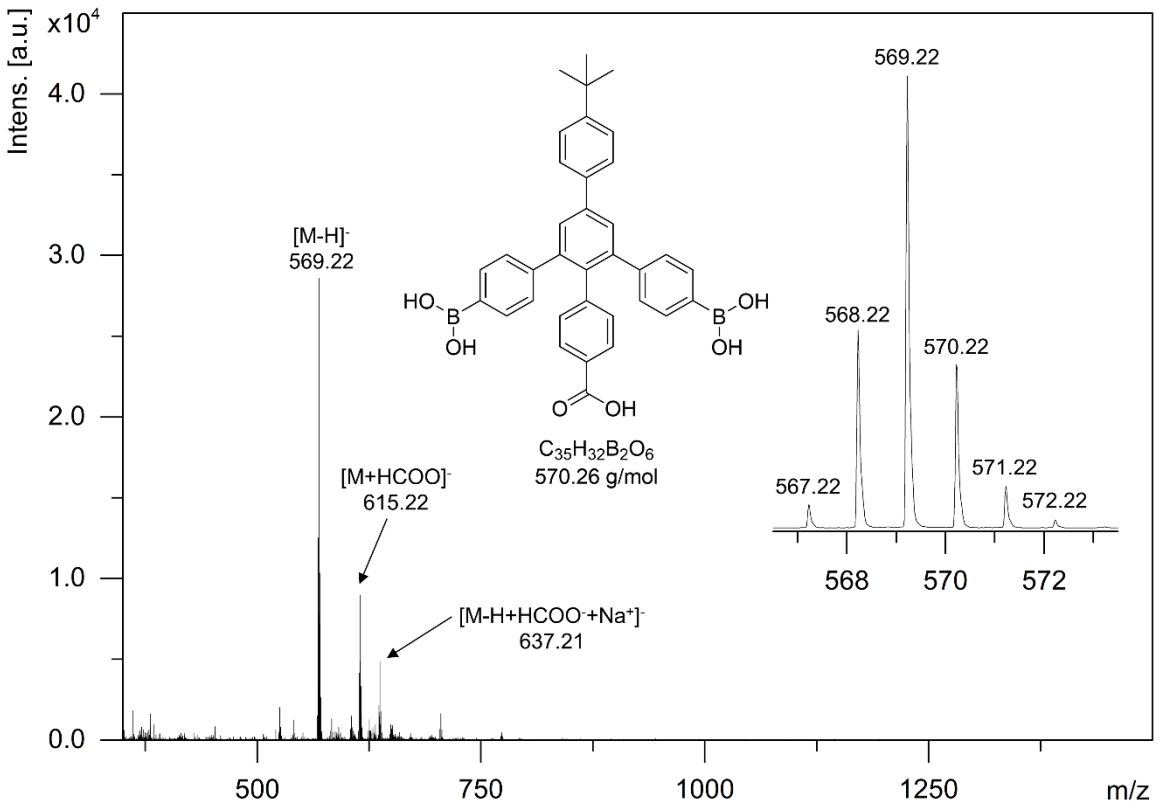

Figure S7. MS (ESI, EtOAc/ACN, neg.) of $\mathbf{C^{PhCOOH}}$.

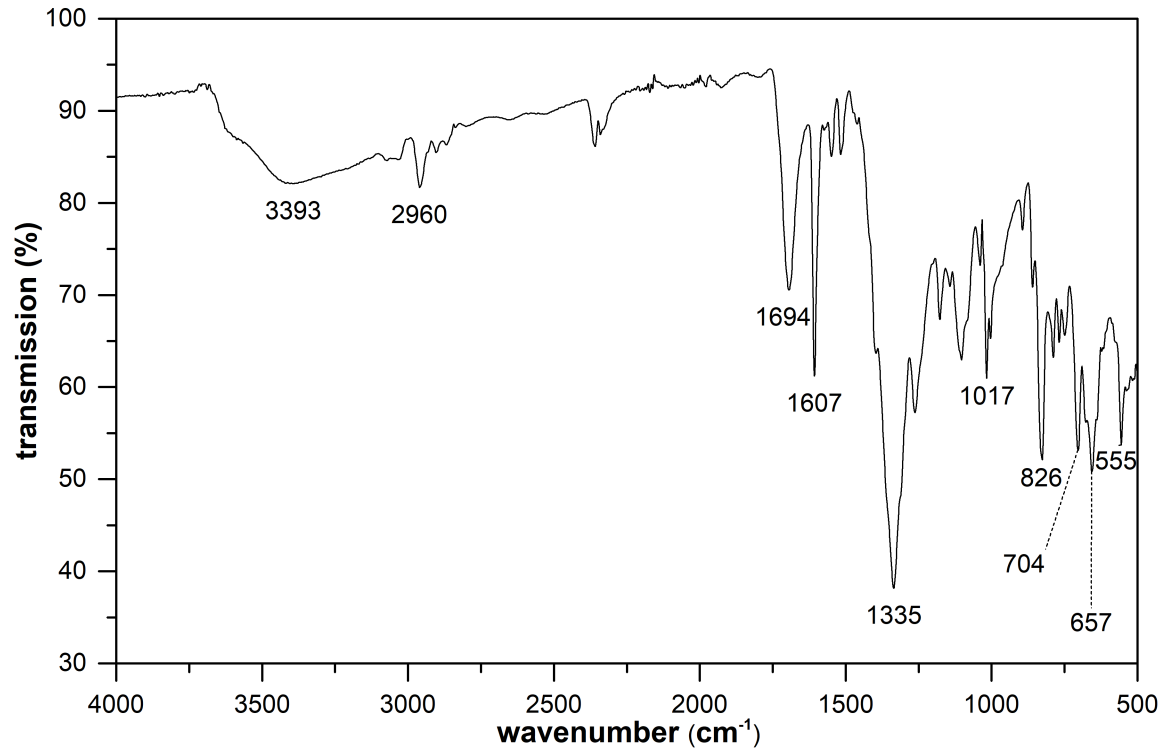

Figure S8. FT-IR spectrum of $\mathbf{C^{PhCOOH}}$.

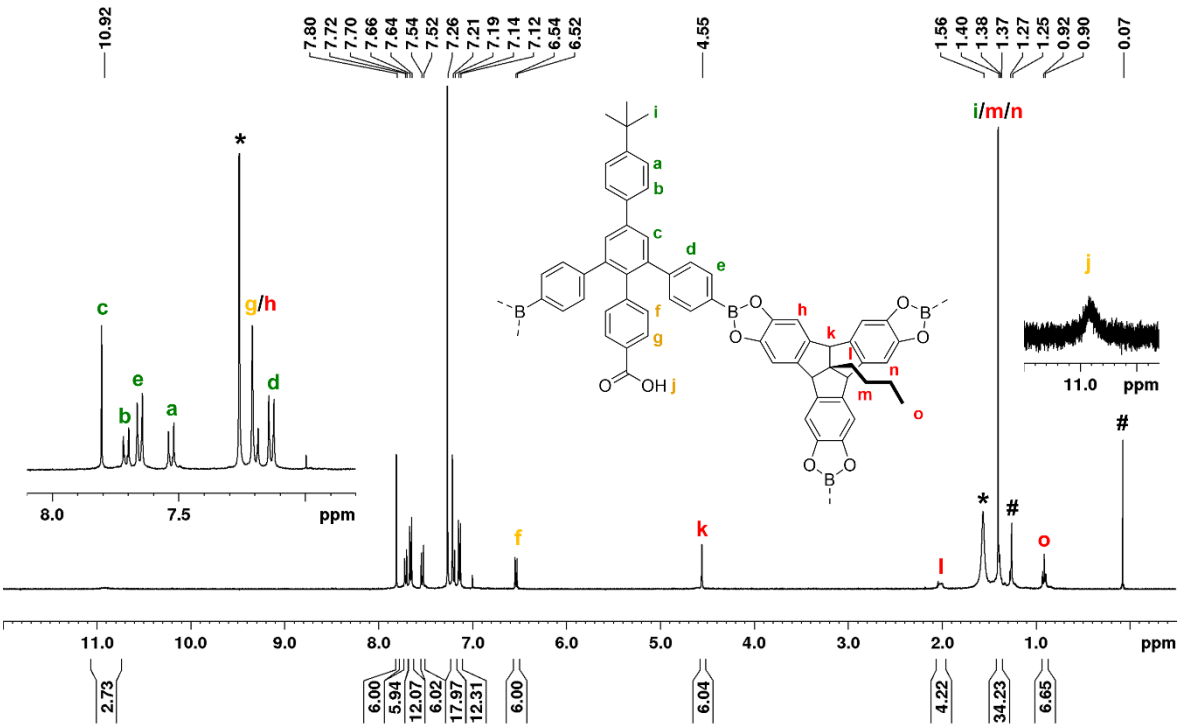

Figure S9. ^{1}H NMR (400 MHz, $CDCl_3$, rt) spectrum of $\mathbf{A_2C^{PhCOOH}_3}$ ($^{\#}$ Indicates grease. * Indicates residual $CHCl_3$ and H_2O).

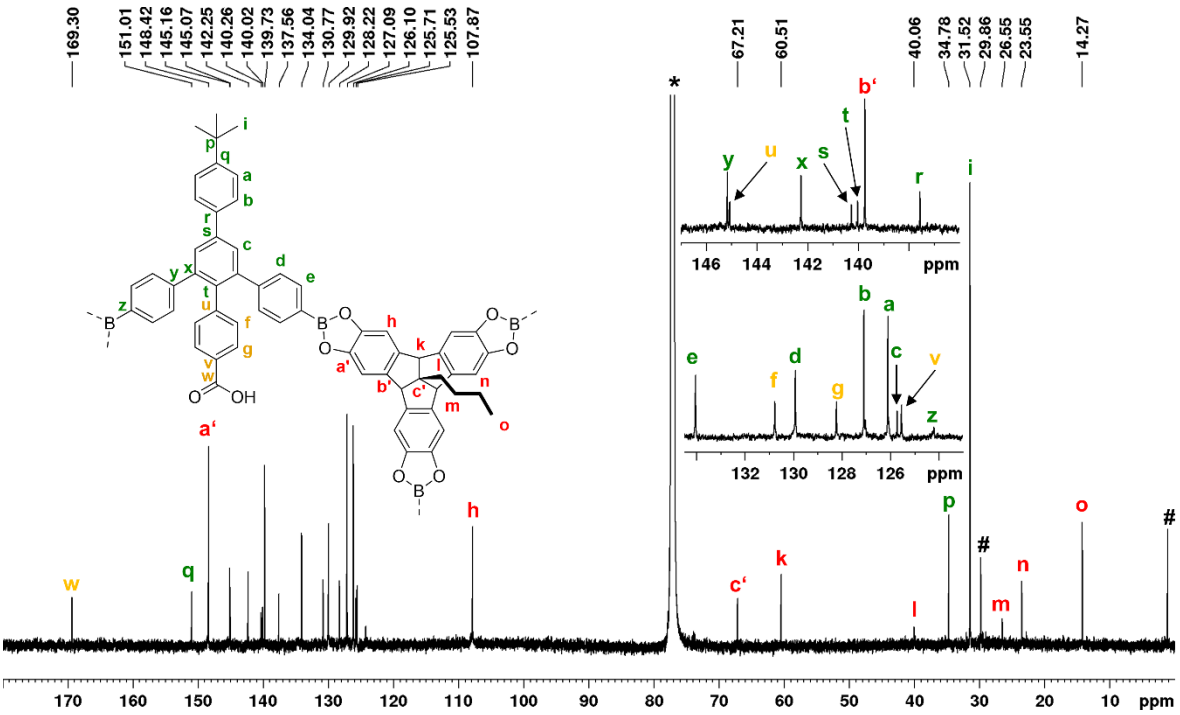

Figure S10. ^{13}C NMR (151 MHz, $CDCl_3$, rt) spectrum of $\mathbf{A_2C^{PhCOOH}_3}$ ($^{\#}$ Indicates grease).

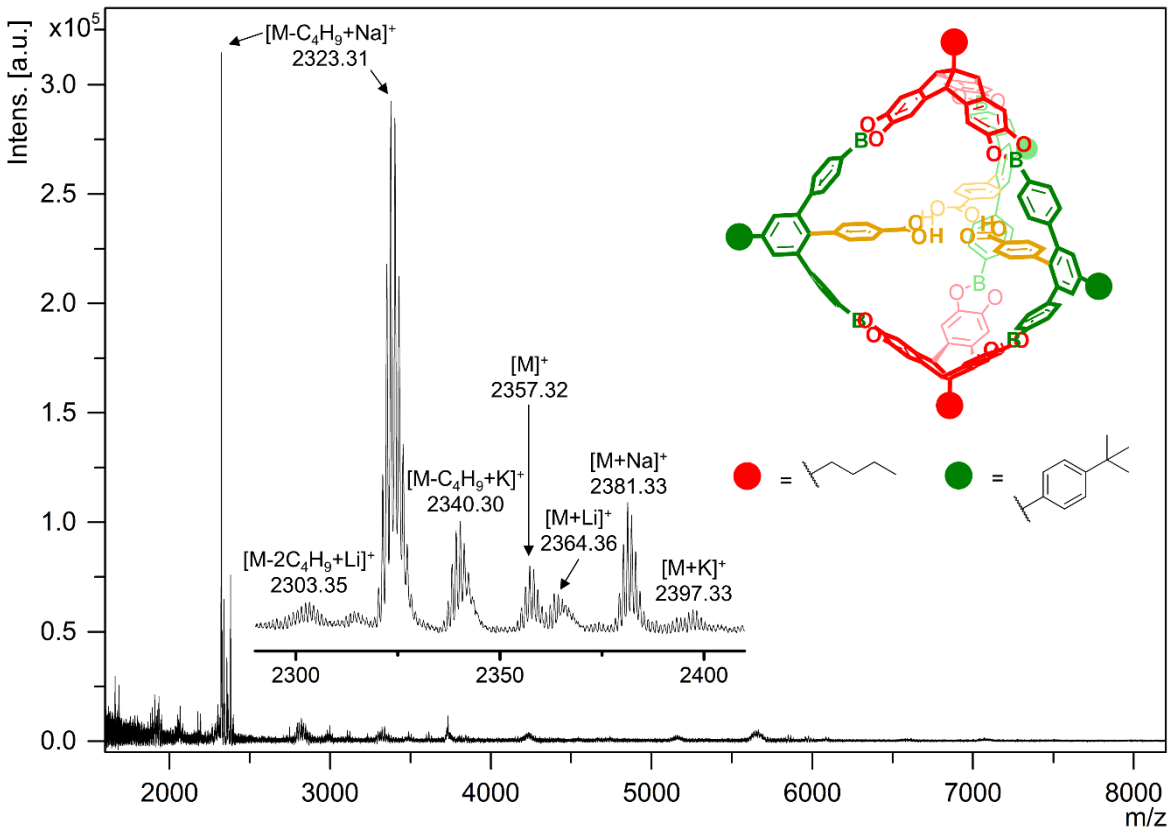

Figure S11. MS (MALDI-TOF, DCTB in $CHCl_3$, pos.) of $\mathbf{A_2C^{PhCOOH}_3}$.

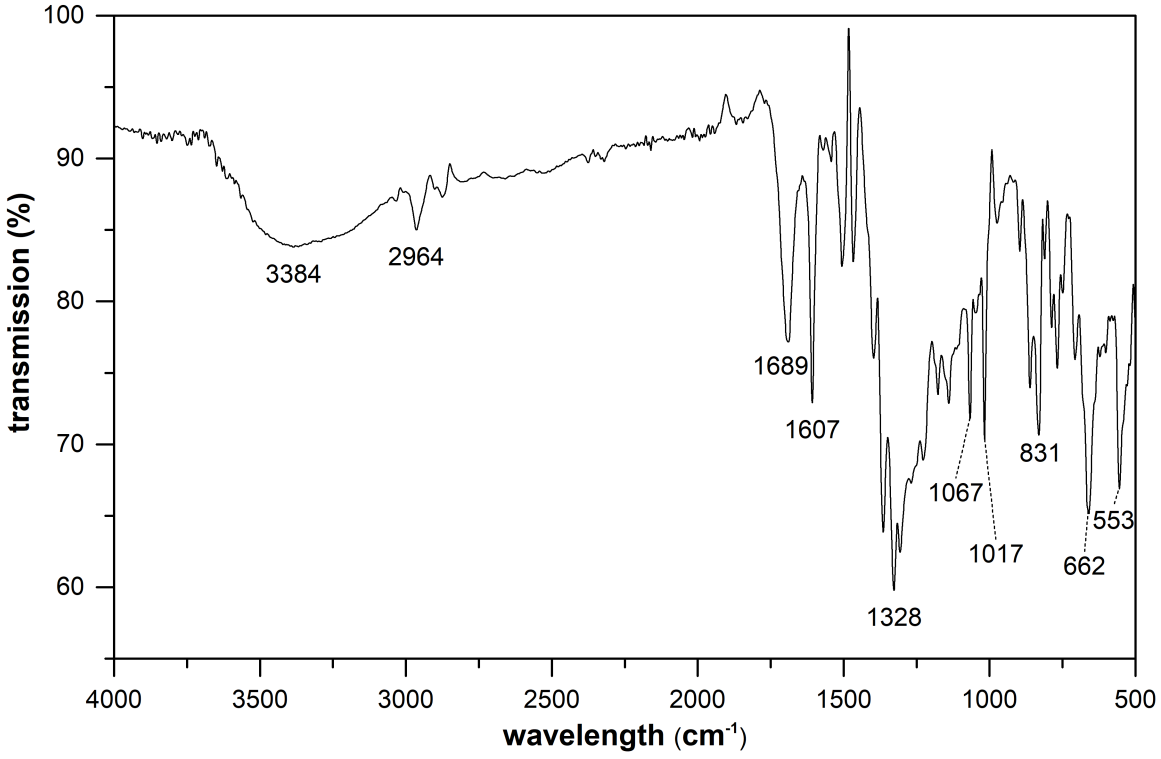

Figure S12. FT-IR spectrum of $\mathbf{A_2C^{PhCOOH}_3}$.

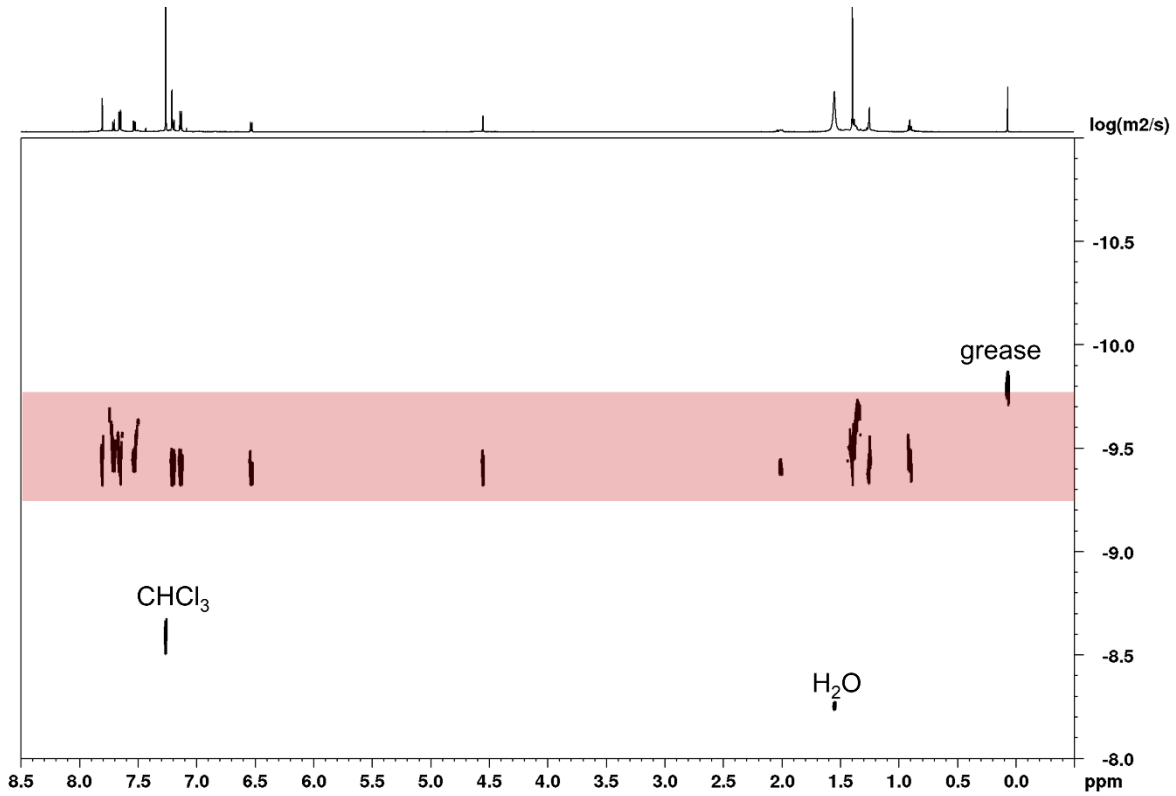

Figure S13. 2D plot of DOSY NMR (600 MHz, CDCl3, 295.6 K) of $\mathbf{A_2C^{PhCOOH}_3}$.

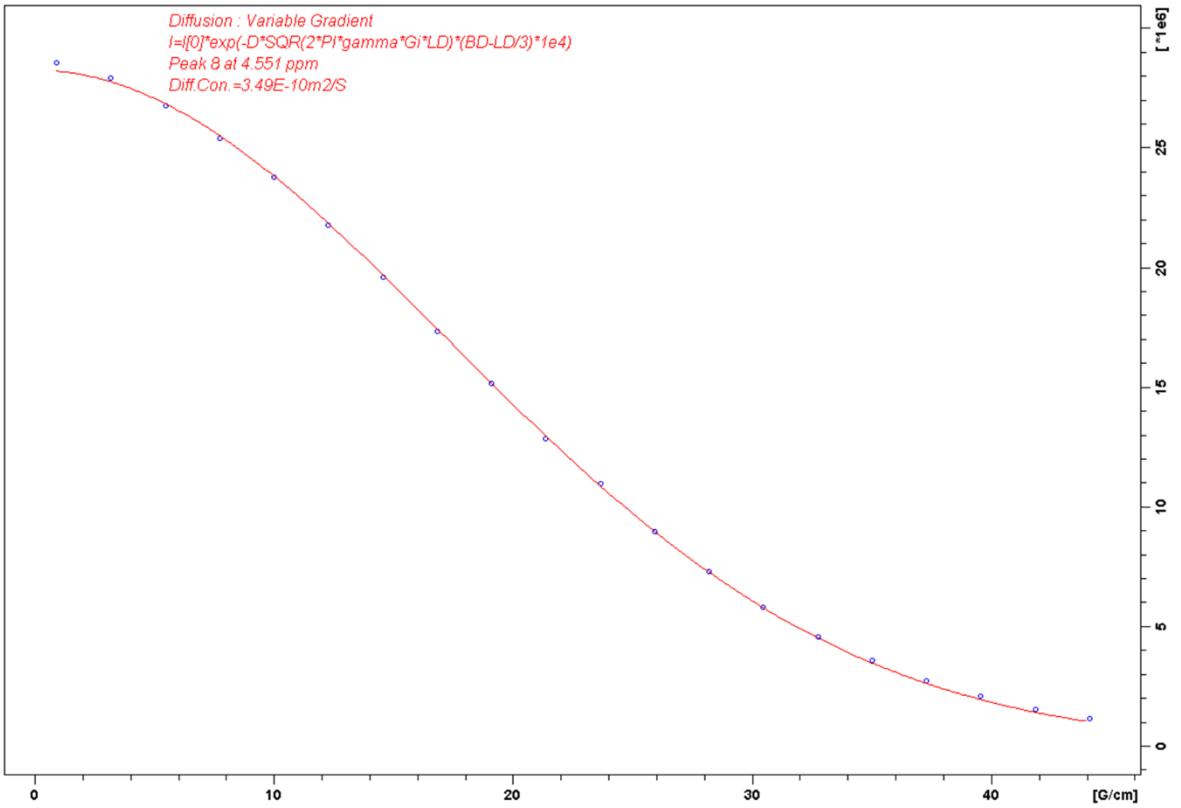

Figure S14. Monoexponential fit of the amplitude decay for selected proton signal at $\delta = 4.56$ ppm of cage $\mathbf{A_2C^{PhCOOH}_3}$.

3 NMR Experiments

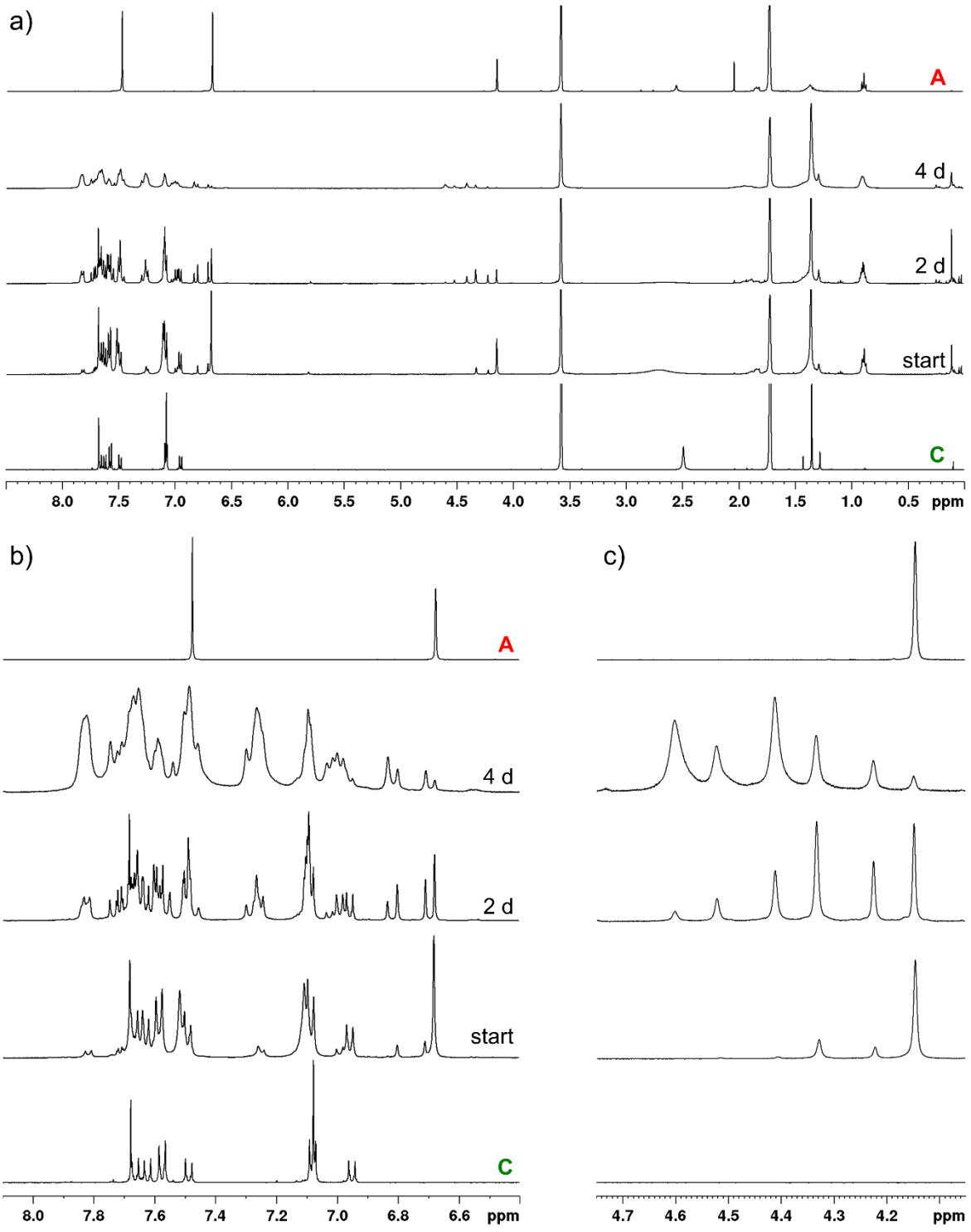

Figure S15. ^{1}H NMR (400 MHz, THF-d_8, rt) spectra of **A**, $\mathbf{C}^{\mathbf{PhCOOH}}$ and the reaction mixture directly, two days and four days after mixing both components (**A**:$\mathbf{C}^{\mathbf{PhCOOH}}$ = 2:3, c(**A**) = 2.5×10^{-2} mol L^{-1}) in THF-d_8: a) overview; b) details of the aromatic region; c) details of the bridgehead area.

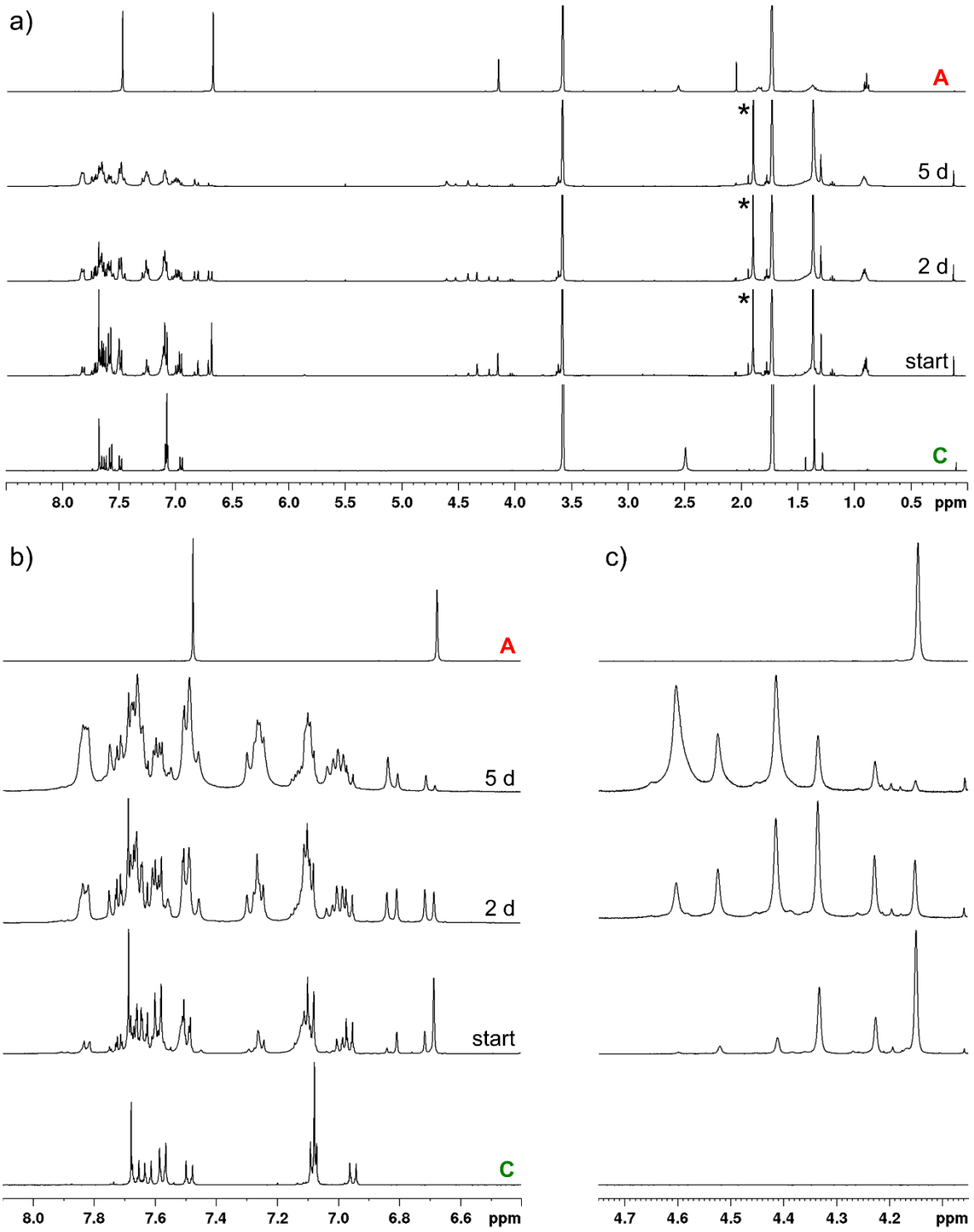

Figure S16. ^{1}H NMR (400 MHz, THF-d_8, rt) spectra of **A**, $\mathbf{C}^{\mathbf{PhCOOH}}$ and the reaction mixture directly, two days and five days after mixing both components in the presence of AcOH (**A**:$\mathbf{C}^{\mathbf{PhCOOH}}$:AcOH = 2:3:6, c(**A**) = 2.5×10^{-2} mol L^{-1}) in THF-d_8: a) overview (* denotes AcOH); b) details of the aromatic region; c) details of the bridgehead area.

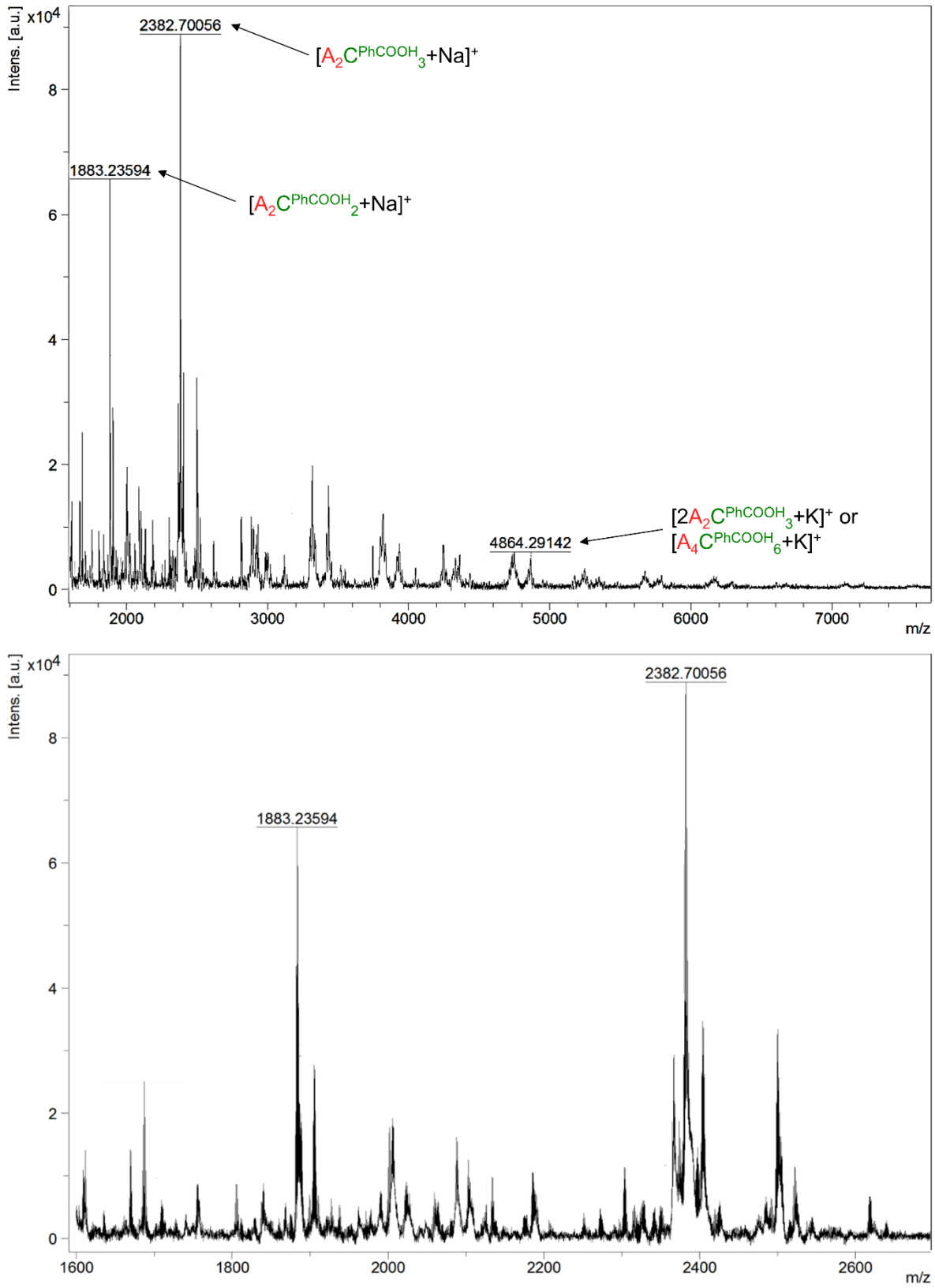

Figure S17. MS (MALDI-TOF, DCTB in $CHCl_3$, pos.) of the reaction mixture from **A**/$\mathbf{C}^{\mathbf{PhCOOH}}$ = 2:3 in THF-d_8 after five days (c(**A**) = 2.5×10^{-2} mol L^{-1}).

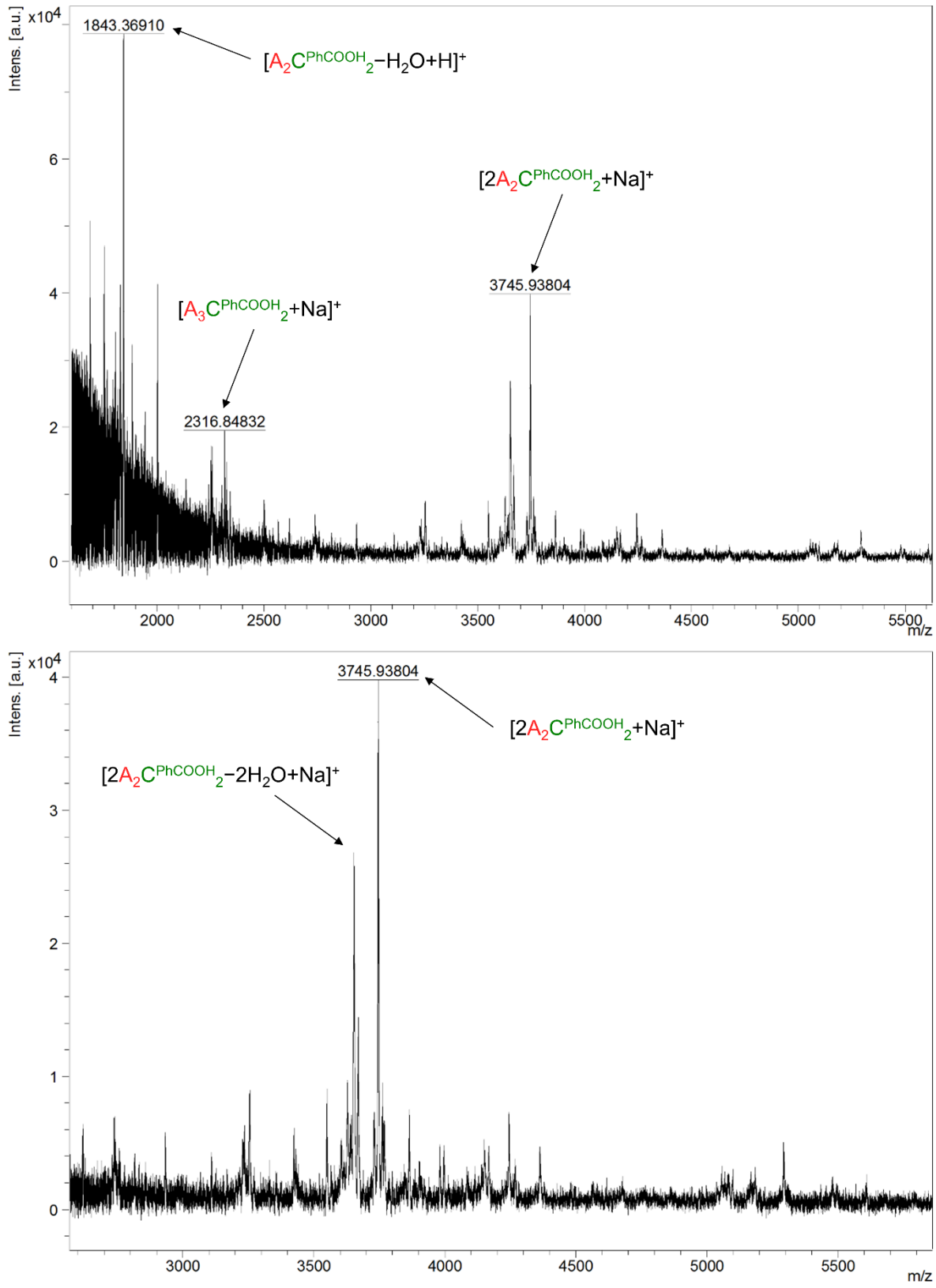

Figure S18. MS (MALDI-TOF, DCTB in $CHCl_3$, pos.) of the reaction mixture from **A**/$\mathbf{C^{PhCOOH}}$ = 2:2 in THF-d_8 after five days (c(**A**) = 2.5×10^{-2} mol L^{-1}).

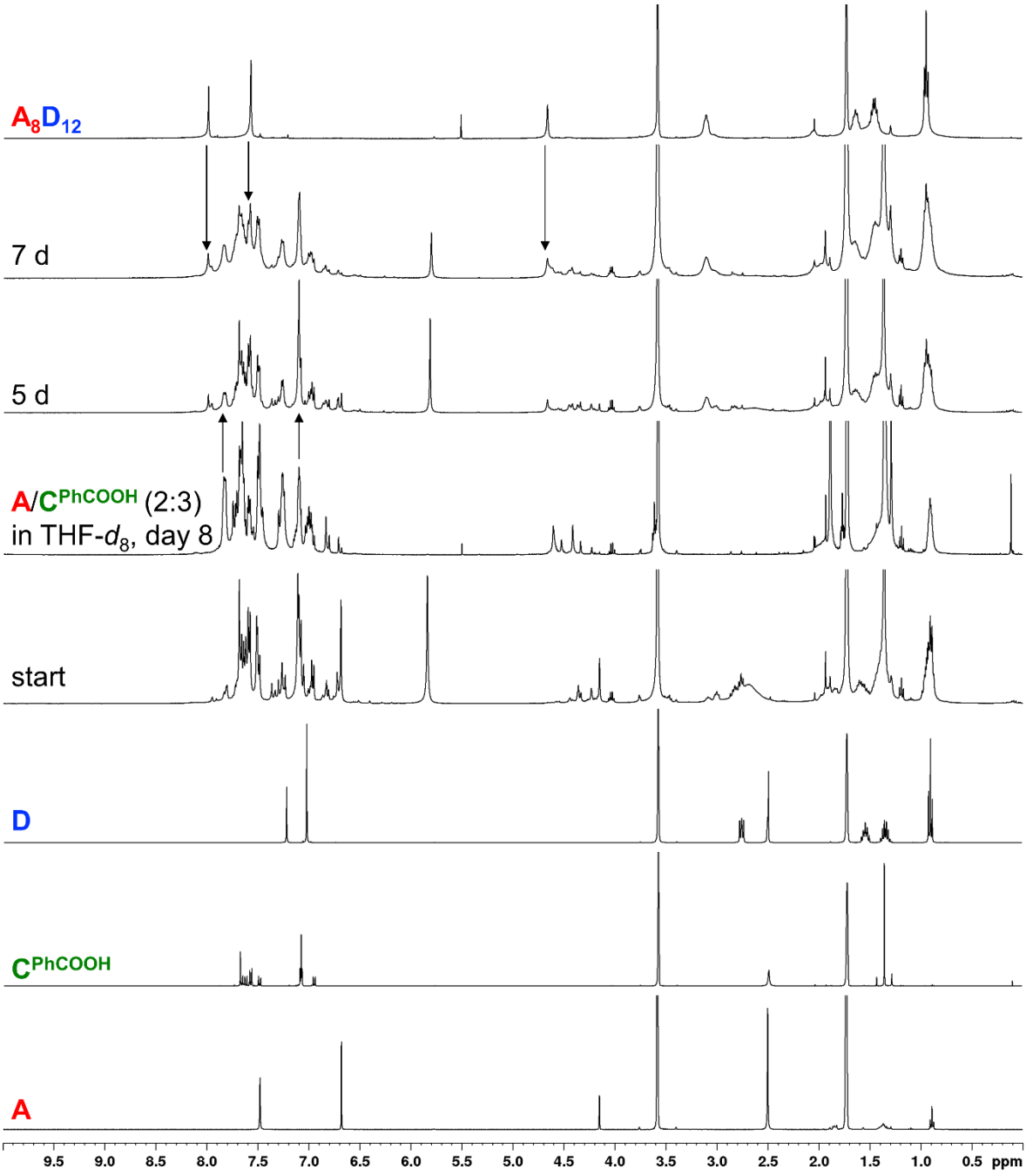

Figure S19. ^{1}H NMR (400 MHz, THF-d_8, rt) spectra for the self-sorting experiment between **A**/**C**$^{\mathbf{PhCOOH}}$/**D** = 4:4:2 (c(**A**) = 2.0×10^{-2} mol L^{-1}) at the beginning of the reaction, after five days and after seven days in comparison to the cubic cage **A**$_8$**D**$_{12}$ and the reaction mixture of **A**$_2$**C**$^{\mathbf{PhCOOH}}_3$ after eight days as well as the starting materials **A**, **C**$^{\mathbf{PhCOOH}}$ and **D**.

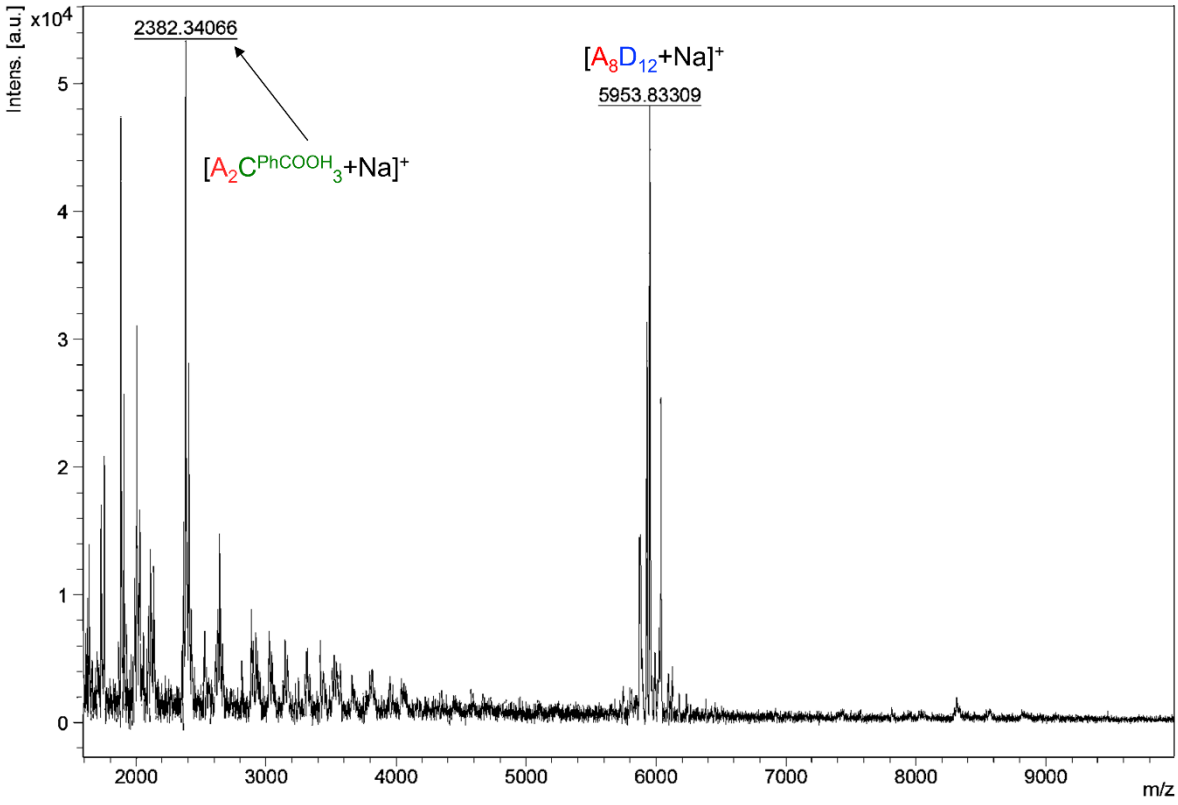

Figure S20. MS (MALDI-TOF, DCTB in $CHCl_3$, pos.) of the reaction mixture for the self-sorting experiment **A**/**C**$^{\mathbf{PhCOOH}}$/**D** = 4:4:2 (c(**A**) = 2.0×10^{-2} mol L^{-1}).

4 Molecular Modeling

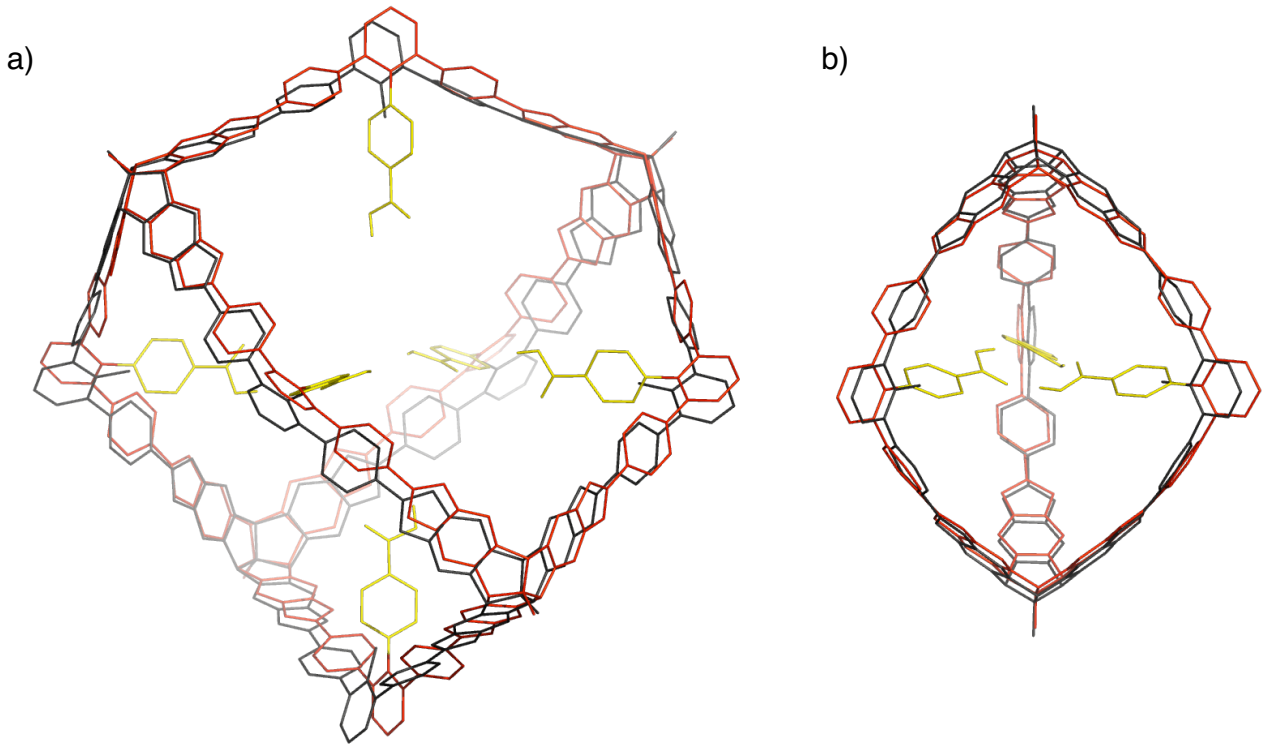

Figure S21. Overlay of DFT-geometry optimized molecular structures for a) tetrahedral cages $\mathbf{A_4C^{Me}_6}$ (black) and $\mathbf{A_4C^{PhCOOH}_6}$ (red, PhCOOH substituents in yellow) and b) trigonal-bipyramidal cages $\mathbf{A_2C^{Me}_3}$ (black) and $\mathbf{A_2C^{PhCOOH}_6}$ (red, PhCOOH substituents in yellow); to reduce computational time and resources, ^{n}Bu groups at the apical position of **A** have been replaced with Me groups and ^{t}BuPh substitutents in 5'-position of $\mathbf{C^{PhCOOH}}$ have been replaced with H atoms; for the images, H atoms are omitted for clarity.

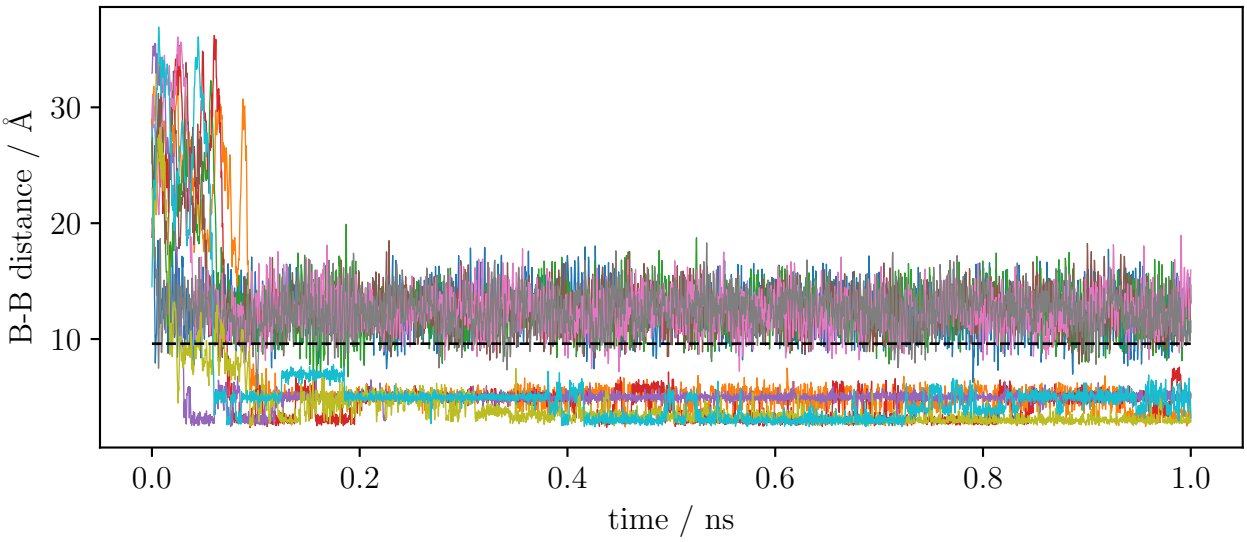

Figure S22. Ten MD trajectories for $\mathbf{AC^{PhCOOH}_2}$ with different starting conformations at 298 K for 1 ns (the dashed black line marks the B-B distance in the $\mathbf{A_2C^{PhCOOH}_2}$ macrocycles).

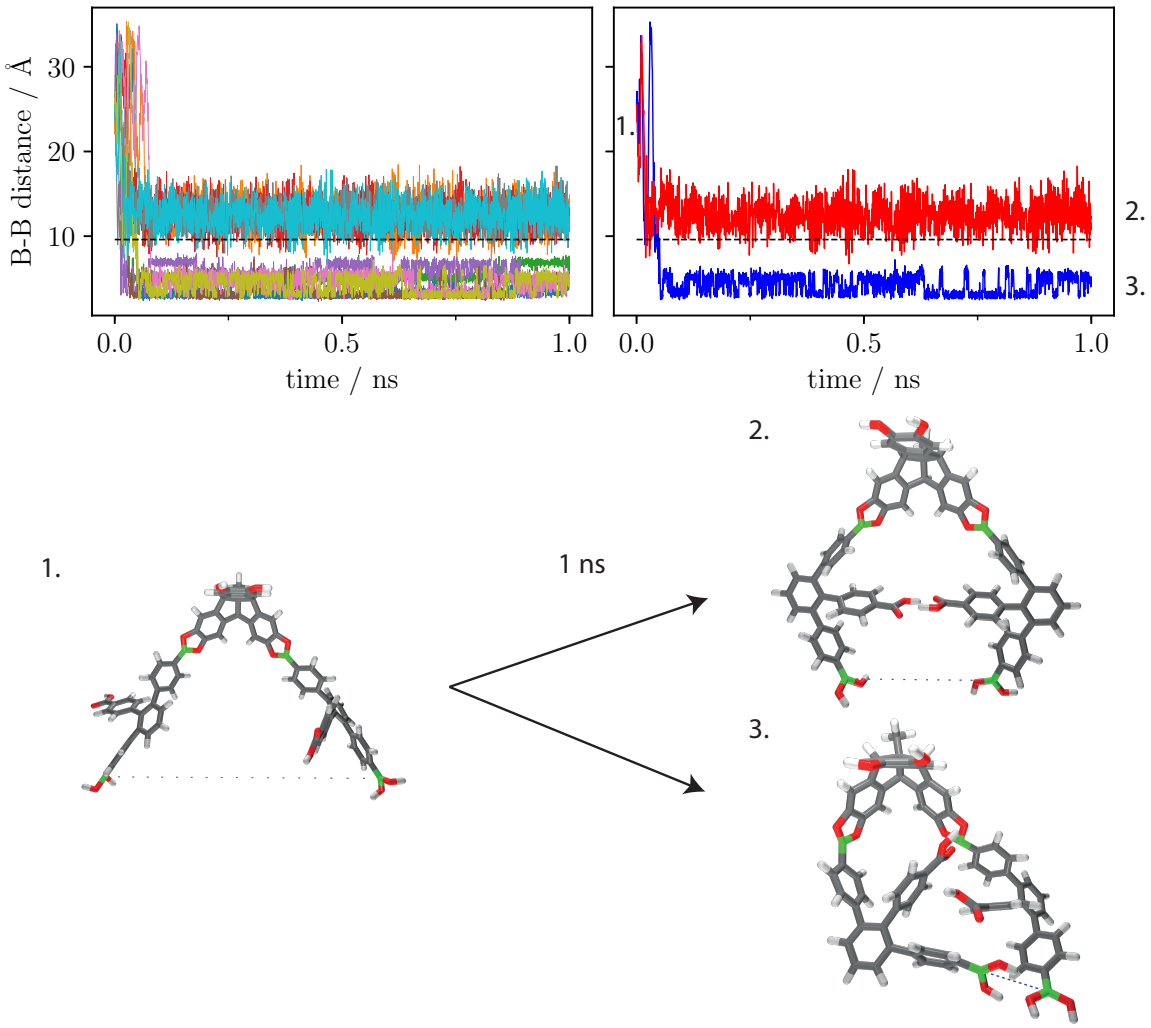

Figure S23. Right: MD trajectories for one starting conformation of $\mathbf{AC^{PhCOOH}_2}$ (1.) with ten randomly generated initial velocities at 298 K for 1 ns (the dashed black line marks the B-B distance in the $\mathbf{A_2C^{PhCOOH}_2}$ macrocycles); left: Two selected trajectories leading to fixed U-shaped conformer (2., red trace) or a more compact metastable conformer (3., blue trace)

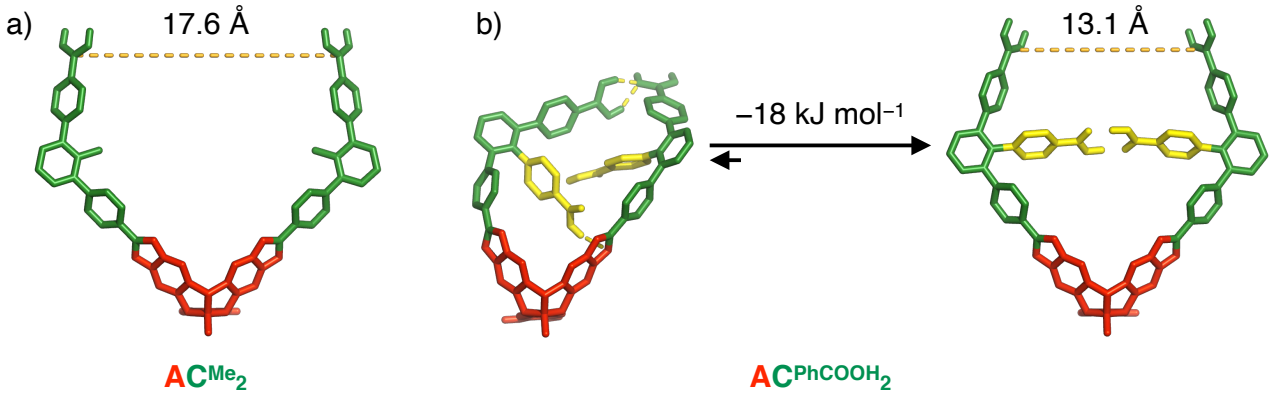

Figure S24. DFT-geometry optimized molecular structures for a) $\mathbf{AC^{Me}_2}$ and b) the two fixed conformers for $\mathbf{AC^{PhCOOH}_2}$ obtained from MD simulations.

5 References

[S1] R. Breslow, P. Marks, A. Mahendran, Y. Yao (Columbia University), US20180118709, **2018**.

[S2] S. Klyatskaya, N. Dingenouts, C. Rosenauer, B. Müller, S. Höger, *J. Am. Chem. Soc.* **2006**, *128*, 3150–3151.

[S3] A. B. Vliegenthart, F. A. L. Welling, M. Roemelt, R. J. M. Klein Gebbink, M. Otte, *Org. Lett.* **2015**, *17*, 4172–4175.

[S4] S. Klotzbach, T. Scherpf, F. Beuerle, *Chem. Commun.* **2014**, *50*, 12454–12457.